



**STUDIES ON BIOSORPTION USING *JANIA RUBENS* RED ALGAE
POWDER OF VICTORIA BLUE DYE**

Dr.Ch. A.I. Raju¹, Dr. M. Tukaram Bai², Prof. P. Rajendra Prasad³ and R. Sateesh⁴

¹Associate Prof, Chemical Engineering Department, Andhra University, Visakhapatnam, AP, India

²Associate Prof, Chemical Engineering Department, Andhra University, Visakhapatnam, AP, India

³Retired Prof, Chemical Engineering Department, Andhra University, Visakhapatnam, AP, India

⁴Research Scholar, Chemical Engineering Department, Andhra University, Visakhapatnam, AP, India

Corresponding Author: Dr. Ch. Asha Immanuel Raju
Email: chairaju@andhrauniversity.edu.in

Abstract

A low-cost, readily available adsorbent was used to remove dye from an aqueous solution in a batch experiment. The ability of the inexpensive adsorbent (*Jania rubens* red algae) to remove Victoria blue dye from an aqueous solution at room temperature was examined. The parameters examined included pH, initial dye concentration, temperature, contact time, isotherms, and kinetics. We looked into how these system variables affected the rate of uptake of dye. Optimization was also carried out using Central Composite Design in Response Surface methodology with STATISTICA software. Characterization was also incorporated using FTIR, XRD and SEM.

Keywords: Biosorption, Dye, Adsorption, RSM, FTIR, SEM.

Introduction

Water, which is one of the abundant compounds found in nature, covers approximately three-fourths of the surface of the earth. Over 97% of the total quantity of water is in the oceans and other saline bodies of water and is not readily available for our use. Over 2% is tied up in polar ice caps and glaciers and in atmosphere and as soil moisture. As an essential element for domestic, industrial and agricultural activities, only 0.62% of water found in fresh water lakes, rivers and groundwater supplies, which is irregularly and non-uniformly distributed over the vast area of the globe, is accessible [1]. Different reports are accessible which show destructive impacts of azo colors on plants (plant development and germination). Due to their impact on groundwater and surface water as well as human health, industrial pollutants are one of the most significant environmental issues [2]. Metallic species brought into the environment by human technology tend to persist indefinitely, circulating and eventually accumulating throughout the food chain, posing a serious threat to humans, animals, and the environment. Realize that the metal can only be "removed" from solution if it is properly immobilized. The strategy of metal expulsion from fluid arrangements frequently prompts successful metal fixation [3]. It has been established that the metal binding mechanism is affected by the functional groups on the

biosorbent and the metal speciation in the solution. According to Nakamoto (1997), infrared spectroscopy is a powerful tool for studying biological molecules. It has been used to obtain structural and bonding information on large and complex molecules. The main focus of this work is on figuring out how certain anionic metal complexes like goldcyanide ($\text{Au}(\text{CN})_2^-$), vanadate (VO_4^{3-}), and chromate (CrO_4^{2-}) bind to the AWUS material [4]. Adsorption is one of the effective, low-cost methods for removing dyes from water. Adsorbents like activated carbon, peat, chitin, clay, and others have been used in adsorption techniques to reduce the concentration of dye in industrial effluents (Tahir, 2005). Adsorption is the process by which chemical or physical bonding holds atoms, molecules, or ions on solid surfaces [5]. This study used soil incubation experiments to compare time-dependent phase distributions of bentazone and its metabolites in the soils from the initial treatment to 160 days after application and simultaneously evaluate bentazone mineralization in three cultivated soils—sandy, loamy, and clay. Release kinetics and desorption isotherms were measured in order to achieve these goals [6]. There are three broad categories of dyes: a) anionic (corrosive, responsive, and direct colors) with negative charge essentially because of (SO_3^-) bunch, (b) cationic (fundamental colors) due to the protonated amine bunch, and (c) nonionic (scatter colors) as per their separation conduct influid arrangements [7]. Biosorption has recently been touted as a less expensive and more efficient method for treating dye-contaminated wastewater. Since activated carbon is a good sorbent, it has been used a lot to treat dye wastewater. Due to its high cost, this sorbent has been limited in use. Therefore, environmental scientists have been extremely concerned about alternative materials that are both inexpensive and efficient. For the purpose of removing dyes from aqueous solutions, a variety of natural sorbents have been examined up to this point. Notwithstanding, there is absence of writing managing the conceivable utilization of almond shell deposits specifically as color sorbent [8]. According to Conrad (2008), cellulosic and lignin-rich plant fibers have a strong tendency to attract and remove heavy metal ions from aqueous solutions. Most of the groups that make up these components of plant fiber are alcohols, aldehydes, ketones, carboxylic, phenolic, and ether groups. These groups are known to bind heavy metals by giving them an electron pair to form complexes or exchange hydrogen ions for heavy metal ions in solution [9].

Experimental Procedure

Reagents and Materials:

This investigation is made of only analytical-grade chemicals. After dissolving one gram of Victoria Blue dye in one thousand milliliters of distilled water, a stock solution containing 1000 mg/L was made, which was then adjusted to various concentrations and pH ranges by adding 0.1M NaOH and 0.1M HCL, the desired pH of the dye solution was achieved.

Preparation of the biosorbent:

Jania rubens red algae was procured from tenneti park near jodugullapalem, visakhapatnam. Algae is washed and dried till the pigmentation totally vanishes and the algae was like dry gramss. After that, these dried alage was finely powdered and sized by going through a set of sieves with mesh sizes ranging from 152 to 53.

Preparation of Victoria Blue dye solution:

By dissolving one gram of Victoria Blue dye in one thousand milliliters of distilled water, a

stock solution containing 1000 mg/L of the dye is created. Analytical reagents and distilled water are used to prepare each and every one of the required solutions. Dilutions of this stock solution are used to create synthetic samples of the dye at various concentrations. In a 1000 mL volumetric flask, 20 mL of 1000 ppm stock solution is diluted to the mark with distilled water to make 20 mg/L stock solution. Additionally, solutions containing dye concentrations ranging from 50 to 200 mg/L are prepared. By adding 0.1M NaOH and 0.1M HCL, the pH of the aqueous solution is brought up to the desired level.

Studies on equilibrium biosorption process:

Analyses of how various parameters affect things like: The characterization (FTIR, SEM), isotherms (Langmuir, Freundlich, Temkin), kinetics (Lagergren first order, Pseudo second order), thermodynamics (Entropy, Enthalpy, and Gibbs Free Energy), and optimization through response surface methodology are all investigated in order to comprehend the biosorption process and reach a conclusion.

Results and Discussion

The biosorption of Victoria Blue dye is investigated in relation to a variety of parameters. The deliberate information comprises of beginning and last centralization of Victoria Blue color, tumult time, biosorbent size, biosorbent measurement, pH of the watery arrangement and temperature of the watery arrangement. Batch experiments are used to get the experimental data. Response Surface Methodology studies involving Central Composite Design and FTIR and SEM characterization studies follow.

Effect of agitation time:

Figure 1 depicts the percentage of VB dye biosorption by Janiarubens red algae and the agitation time. In initial 20 min of fomentation the 38% biosorption is slowly expanded and their plots are found and the biosorption is pretty much consistent. As a result, the equilibrium agitation time is 40 minutes with 65 percent biosorption. The dye uptake ranges from 0.2 to 1.3 mg/g during the agitation time period of 5 to 180 minutes, when 50 mol of aqueous solution is added to 10g/L of 53 m size biosorption. This increases the percentage of biosorption from 10% to 65% during the agitation time period of 5 to 40 minutes. At first, the percent rate of biosorption is higher. It remains high because *Jania Rubens* red algae have equal surface area available for the biosorption of VB dye [10-11].

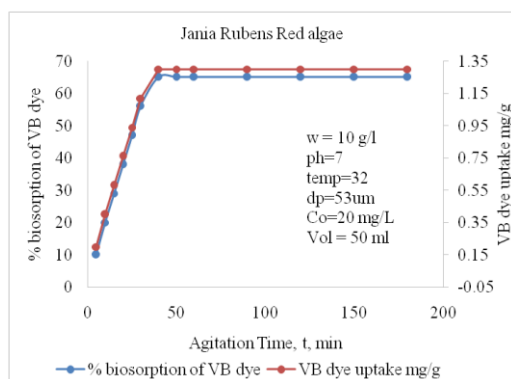


Figure 1: Effect of agitation time on % biosorption of VB dye

Effect of biosorbent size:

The image above The variation in the percentage of VB dye that is bioabsorbed by *Jania Rubens* red algae and its biosorbent size is depicted in Figure 2. The dye uptake ranges from 1.3 to 0.82 mg/g, and the biosorbent surface area increases as the particle size decreases as the biosorbent size increases from 53 to 152 m. The number of biosorbent's active sites are better exposed to the biosorbate [12-13].

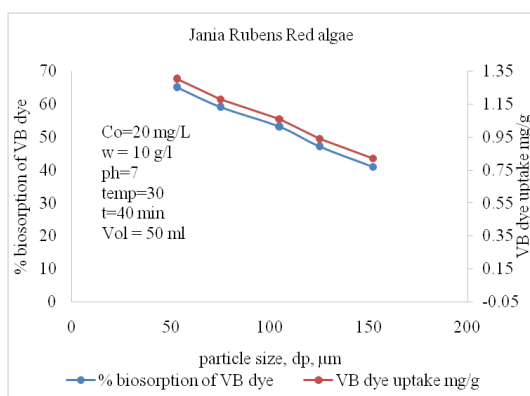


Figure 2: Effect of biosorbent size on % biosorption of VB dye

Effect of pH in aqueous solution:

The plot below shows the relationship between *Jania Rubens* red algae's biosorption VB dye and the pH of an aqueous solution. According to figure 3 as pH rises from 2 to 6 (from 49 to 72 percent), the percentage of biosorption increases significantly, and the percentage of biosorption decreases after pH 6. A typical experiment involves adding a biosorbent dosage of 10g/L of 53 m size to 50 ml of aqueous solution, which results in an increase in biosorption from 49 to 52 percent and dye uptake from 0.98 to 1.040 in the pH range of 2 to 8. The obtained result suggests that the ions may have exchanged chemical interactions. The presence of SO₃ stretching, S=O, and C-S-O bands from ester sulfonate groups is extremely rich due to the involvement of ion exchange in biosorption [14-15].

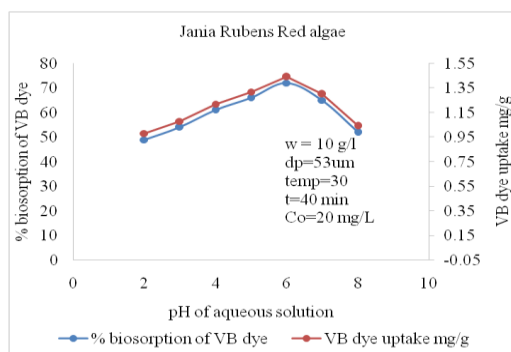


Figure 3: Effect of pH on % biosorption of VB dye

Effect of initial concentration of VB dye by *Jania rubens* red algae:

The percentage of biosorption at equilibrium agitation time is shown to be influenced by the initial concentration of VB dye that *Janiarubens* red algae in the aqueous solution. While

increasing the concentration of VB dye by *Jania Rubens* red algae from 20 to 200 mg/L in an aqueous solution, the percentage of VB dye by *Jania Rubens* red algae that is removed from higher concentrations of VB dye by *Jania rubens* red algae gradually decreases from 72 to 52% (1.44 to 10.40 mg/g). The accessible dynamic locales on the biosorbent expansions in how much biosorbate to the perpetual is the way of behaving noticed [16-17].

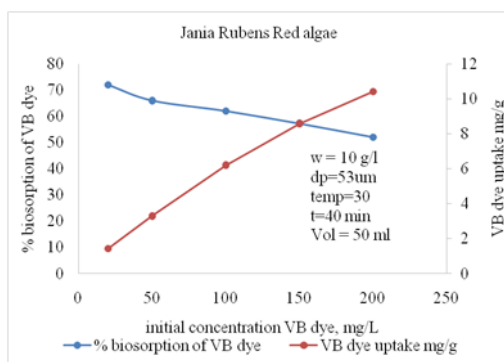


Figure 4: Effect of initial concentration for the biosorption of VB dye

Effect of biosorbent dosage:

The figure 5 represents the amount of biosorbent in an aqueous solution and the variation in the percentage of VB dye that is bioabsorbed by *Jania rubens* red algae. The percentage of biosorption is increased from 72 to 89.5%, and the dosage is increased from 10 to 70 g/L. The dose ranged from 10 g/L (or 72%), to 30 g/L (or 85%). The percentage of biosorption increased slightly from 30 to 50 g/L, but not significantly (89 to 89.5%). This is because there is more biosorbent, which would increase the number of dye-uptake-friendly active sites [18-19].

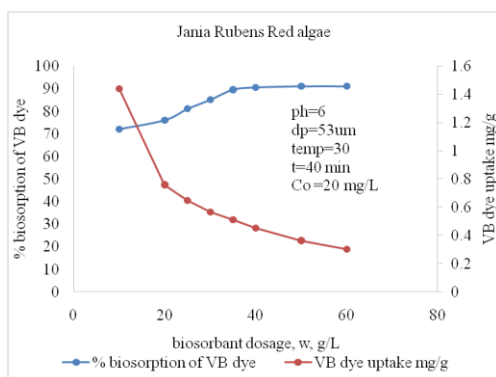


Figure 5: Effect of biosorbent dosage on % biosorption of VB dye

Effect of temperature:

The equilibrium dye uptake was significantly affected by temperature. The figure 6 shows the impact of changes in the temperature on the VB color take-up. The graph shows that the adsorption capacity of *Jania rubens* red algae for the VB dye increased with temperature. In addition to the temperature, an increase in the large dye ion's mobility, from 283K (84 percent) to 323K (90.5 percent), may be the cause. The ideal temperature was found to be 303 K, or 89.5 percent. Dynamic destinations at the surface go through an association by expanding number of

particles may likewise required energy. Further the inner design *Jania rubens* red algae enabling enormous colors to enter with the temperature expanding which might create an enlarging outcome [20-21].

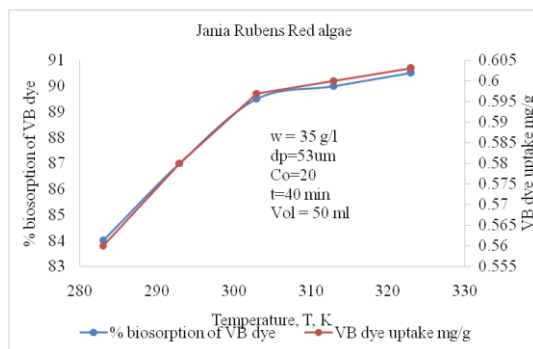


Figure 6: Effect of temperature on % biosorption of VB dye

Isotherms:

Langmuir isotherm:

Langmuir isotherm is the most widely used simple two- parameter equation. This simple isotherm is based on following assumptions:

- ✓ Adsorbate is chemically adsorbed at a fixed number of well- defined sites.
- ✓ Each site can hold only one adsorbate species.
- ✓ All sites are energetically equivalent.
- ✓ There are no interactions between the adsorbate species.

The Langmuir relationship is hyperbolic and the equation is:

$$q_e/q_m = K_L C_e / (1 + K_L C_e) \quad \text{-----}(3.1)$$

The above equation can be rearranged as

$$(C_e/q_e) = 1/(K_L q_m) + C_e/q_m \quad \text{-----} (3.2)$$

From the plots between (C_e/q_e) and C_e , the slope $\{1/(K_L q_m)\}$ and the intercept $(1/q_m)$ can be calculated. Further analysis of Langmuir equation can be made on the basis of separation factor $[R_L = 1/(1 + K_L C_e)]$.

$0 < R_L < 1$ indicates favorable adsorption

$R_L > 1$ indicates unfavorable adsorption

$R_L = 1$ indicates linear adsorption

$R_L = 0$ indicates irrepressible adsorption

Langmuir isotherm is drawn between C_e/q_e and C_e in fig. 3.7 for the present data. The resulting equation is

$$(C_e/q_e) = 0.0562 C_e + 3.8942 \quad \text{-----} (3.3)$$

The (correlation coefficient of 0.9879) confirms strong binding of VB dye ions to the surface of *Jania rubens* red algae [22-23].

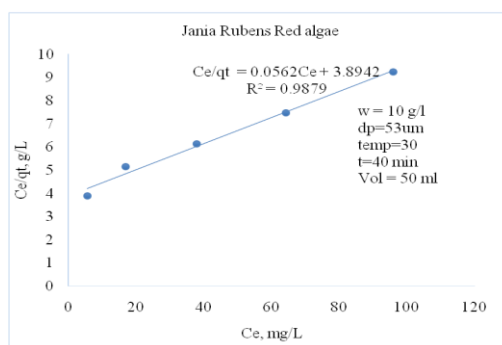


Figure 7: Langmuir isotherm for biosorption

Freundlich isotherm:

Freundlich introduced an exact adsorption isotherm condition that can be applied in case of low and transitional fixation ranges.

The Freundlich isotherm can be obtained from

$$q_e = K_f C_e^n \quad \text{----- (3.4)}$$

Where K_f , mg/g represents the adsorption capacity at dye equilibrium concentration and n represents the degree of dependence of adsorption.

Taking LN on both sides, we get

$$\ln q_e = \ln K_f + n \ln C_e \quad \text{----- (3.5)}$$

Freundlich isotherm is drawn between $\ln C_e$ and $\ln q_e$ in fig. 5.8, resulted in the following equation

$$\ln q_e = 0.7093 \ln C_e - 0.8252 \quad \text{----- (3.6)}$$

The equation has a correlation coefficient of 0.9956. The 'n' value of 0.7093 indicates favorable biosorption satisfying the condition of $0 < n < 1$ [24-25].

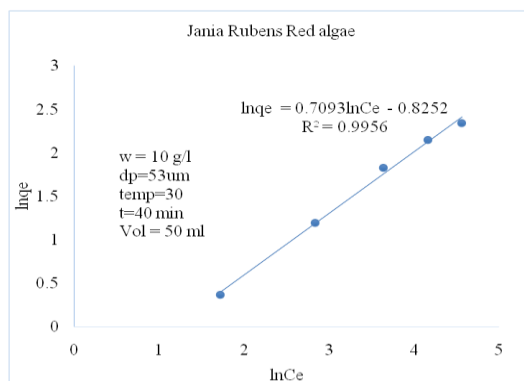


Figure 8: Freundlich isotherm for biosorption

Temkin isotherm:

Temkin and Pyzhev isotherm equation describes the behavior of many adsorption systems on heterogeneous surface and is based on the equation:

$$q_e = RT \ln(A_T C_e) / b_T \quad \text{----- (3.7)}$$

The linear form of Temkin isotherm is

$$q_e = (RT / b_T) \ln(A_T) + (RT / b_T) \ln(C_e) \quad \text{----- (3.8)}$$

Where $A_T = \exp [b (0) \times b (1) / RT]$

Slope, $b (1) = RT / b_T$

Intercept, $b(0) = (RT/b_T) \ln(A_T)$

Plot between q_e and $\ln C_e$ is shown in fig. 3.9. The equation for VB dye biosorption is

$$q_e = 3.183 \ln C_e - 4.7872 \text{ ----- (3.9)}$$

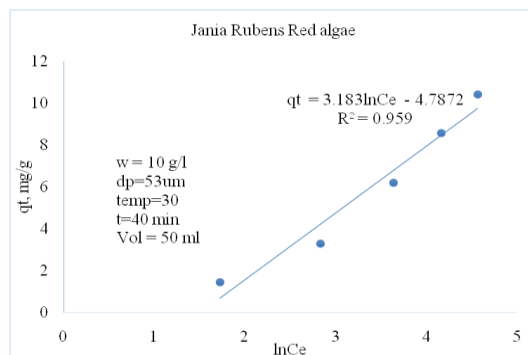


Figure 9: Temkin isotherm for biosorption

The isotherm constants are compiled in table-1. It is found that biosorption data are well represented by Langmuir isotherm ($R^2=0.9879$), Temkin ($R^2=0.959$) and Freundlich isotherms ($R^2=0.959$) [27-28].

Table 1. Isotherm constants

Langmuir isotherm	Freundlich isotherm	Temkin isotherm
$q_m = 17.79 \text{ mg/g}$	$K_f = 0.3186 \text{ mg/g}$	$A_T = 0.17696 \text{ L/mg}$
$K_L = 0.01137$	$n = 0.7093$	$b_T = 876.176$
$R^2 = 0.9879$	$R^2 = 0.9956$	$R^2 = 0.959$

Kinetics:

Lagergren first order:

Lagergren plot and pseudo second order kinetics plot for biosorption of VB dye are drawn in figs. 10 & 11. Table-2 summarizes the rate constant values for first and second order rate equations[28-29]. It is noted that both first and second order rate equations explain the biosorption interactions satisfactorily.

$$\log(q_e - q_t) = -0.03 t + 0.2574, R^2 = 0.9396$$

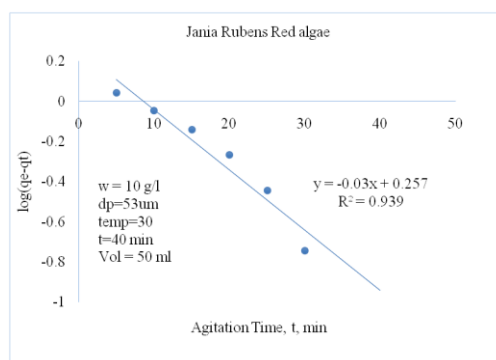


Figure 10: First order kinetics for biosorption

Pseudo second order:

Second order rate equations explain the biosorption interactions satisfactorily[30-31]. The rate constant values for second order rate equations

$$t/q_t = 0.081 t + 24.509, R^2=0.9378$$

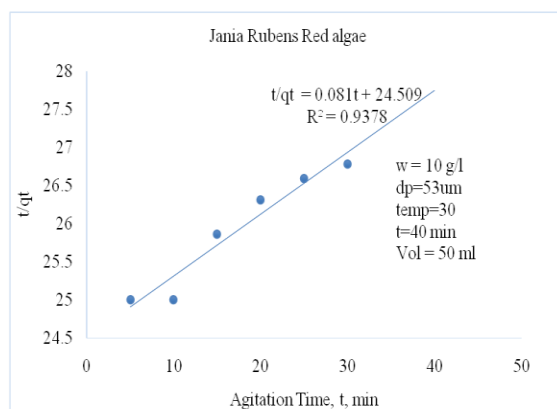


Figure 11: Second order Kinetics for biosorption

Table 2: Equations and rate constants

Order	Equation	Rate constant	R ²
Lagergren first order	$\log (q_e - q_t) = -0.03 t + 0.2574$	0.0552 min^{-1}	0.939
Pseudo second order	$t/q_t = 0.081 t + 24.509$	$0.0857 \text{ g/ (mg-min)}$	0.9378

Thermodynamics:

Van'tHoff's plot is drawn in figure 12. From the data, Gibbs free energy change (ΔG) is calculated to be -4720.05 J/mol for biosorption of VB dye. The negative ΔG value indicates thermodynamically feasible and spontaneous nature of biosorption. The ΔH parameter is 8.36672 kJ/mol.K . The negative ΔH indicates the endothermic nature of biosorption. ΔS parameter is found to be 15.35199 J/mol K for VB dye biosorption[32-33]. The positive ΔS value suggests an increase in the randomness at the solid /solution interface during Biosorption.

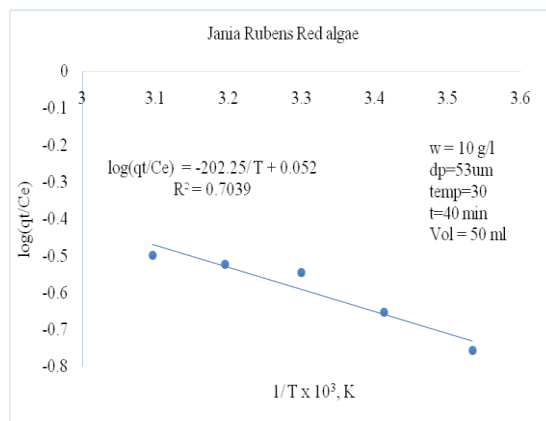


Figure 12. Vant Hoff's plot for Biosorption

Optimization using Response Surface Methodology (RSM):

Optimization using CCD

The parameters that have greater influence over the response are to be identified so as to find the optimum condition for the biosorption of VB dye. The quadratic model is used in the present study, to relate four independent variables and percentage biosorption of VB dye. The regression equation for is % biosorption of VB dye is function of pH (X_1), C_o (X_2), w (X_3) and T (X_4)[34-35].

The variations in the corresponding coded values of four parameters and response are presented in table-3.

Table-3. Levels of different process variables in coded and un-coded form for % biosorption of VB dye using *Jania rubens* red algae

Variable	Name	Range of Levels				
		-2	-1	0	1	2
X1	pH of aqueous solution	4	5	6	7	8
X2	Initial concentration, C_o , mg/L	10	15	20	25	30
X3	Biosorbent dosage, w , g/L	10	20	30	40	50
X4	Temperature, T , K	283	293	303	313	323

The following equation represents multiple regression analysis of the experimental data for the biosorption of VB dye:

$$Y = -2895.95 + 63.86X_1 + 7.16X_2 + 2.70X_3 + 17.82 X_4 - 5.95X_1^2 - 0.18X_2^2 - 0.04X_3^2 - 0.03X_4^2 + 0.06X_1X_2 + 0.01X_1X_3 - 0.01X_1X_4 - 0.00 X_2X_3 - 0.00 X_2X_4 - 0.00 X_3X_4 \text{----- (3.10)}$$

Table 4: Results from CCD for VB dye biosorption by *Jania rubens* red algae

Run No.	X_1 , pH	X_2 , C_o	X_3 , w	X_4 , T	% biosorption of VB dye	
					Experimental	Predicted
1	5	15	20	293	72.28	72.27
2	5	15	20	313	74.52	74.55
3	5	15	40	293	74.48	74.56
4	5	15	40	313	76.62	76.60
5	5	25	20	293	70.22	70.20
6	5	25	20	313	72.22	72.23
7	5	25	40	293	71.52	71.51
8	5	25	40	313	73.28	73.31
9	7	15	20	293	74.88	74.89
10	7	15	20	313	76.62	76.59
11	7	15	40	293	77.52	77.47
12	7	15	40	313	78.88	78.94
13	7	25	20	293	74.12	74.11

14	7	25	20	313	75.62	75.57
15	7	25	40	293	75.72	75.73
16	7	25	40	313	76.98	76.95
17	4	20	30	303	65.12	65.07
18	8	20	30	303	71.28	71.33
19	5	10	30	303	76.12	76.08
20	6	30	30	303	71.98	72.02
21	6	20	10	303	74.38	74.42
22	6	20	50	303	78.12	78.08
23	6	20	30	283	78.62	78.62
24	6	20	30	323	82.12	82.12
25	6	20	30	303	92.00	92.00
26	6	20	30	303	92.00	92.00
27	6	20	30	303	92.00	92.00
28	6	20	30	303	92.00	92.00
29	6	20	30	303	92.00	92.00
30	6	20	30	303	92.00	92.00

Experimental conditions [Coded Values] and observed response values of central composite design with 2^4 factorial runs, 6- central points and 8- axial points. Agitation time fixed at 50 min and biosorbent size at 53 μm

Table 5 represents the results obtained in CCD. Response obtained from regression in eq.3.10 in the form of ANOVA is presented. From the Fisher's F -test ($F_{\text{model}}= 38160$) and a very low probability value ($P_{\text{model}>F}=0.000000$), it is known from table-5 that the model is highly significant. At 5% level, the computed F -value ($F_{0.05 (14,15)} = \text{MS}_{\text{model}}/\text{MS}_{\text{error}} = 38160$) is greater than that of the tabular F -value ($F_{0.05 (14,15)} \text{ tabulars} = 2.42$), indicating that the treatment differences are significant.

Table 5: ANOVA of VB dye biosorption for entire quadratic model

Source of variation	SS	Df	Mean square(MS)	F-value	$P > F$
Model	1713.298	14	122.37	63404	0.00000
Error	0.029	15	0.00193		
Total	1713.327				

df- degree of freedom; SS- sum of squares; F- factor F; P - probability
 $R^2=0.99999$; $R^2(\text{adj}):0.99998$:

Table 6: Estimated regression coefficients for the VB dye biosorption onto *Jania rubens* red algae

Terms	Regression coefficient	Standard error of the coefficient	t-value	P-value
Mean/Intercept	-2895.95	8.164825	-354.686	0.000000
Dosage, w, g/L (L)	63.86	0.349769	182.566	0.000000
Dosage, w, g/L (Q)	-5.95	0.008439	-705.067	0.000000
Conc, Co, mg/L (L)	7.16	0.069534	102.983	0.000000
Conc, Co, mg/L (Q)	-0.18	0.000338	-531.763	0.000000
pH (L)	2.70	0.034603	77.898	0.000000
pH (Q)	-0.04	0.000084	-466.588	0.000000
Temperature, T, K (L)	17.82	0.051741	344.411	0.000000
Temperature, T,K (Q)	-0.03	0.000084	-344.535	0.000000
1L by 2L	0.06	0.002210	29.414	0.000000
1L by 3L	0.01	0.001105	6.788	0.000006
1L by 4L	-0.01	0.001105	-12.897	0.000000
2L by 3L	-0.00	0.000221	-21.947	0.000000
2L by 4L	-0.00	0.000221	-5.430	0.000070
3L by 4L	-0.00	0.000110	-5.430	0.000070
^a insignificant ($P \geq 0.05$)				

$$Y = -2895.95 + 63.86X_1 + 7.16X_2 + 2.70X_3 + 17.82 X_4 - 5.95X_1^2 - 0.18X_2^2 - 0.04X_3^2 - 0.03X_4^2 + 0.06X_1X_2 + 0.01X_1X_3 - 0.01X_1X_4 - 0.00 X_2X_3 - 0.00 X_2X_4 - 0.00 X_3X_4 \text{----- (3.11)}$$

The larger the value of t and smaller the value of P , the more significant is the corresponding coefficient term. The 't' and 'P' values are analyzed from table-6. It is found that the X_1 , X_2 , X_3 , X_4 , X_1^2 , X_2^2 , X_3^2 , X_4^2 , X_1X_2 , X_1X_3 , X_2X_3 and X_2X_4 have high significance to explain the individual and interaction effect of independent variables on VB dye biosorption. The other terms (X_1X_2 , X_1X_4 , X_2X_3 , X_2X_4 and X_3X_4) are insignificant and are not required to explain biosorption. A synergistic effect is indicated by positive sign of the coefficient which means response increases with an increase in effect, while an antagonistic effect is indicated by a negative sign which means response decreases with an increase in effect. In the observed response values, a measure of the model's variability is provided by the correlation coefficient (R^2). In the present study, the value of the regression coefficient ($R^2 = 0.9999$) for eq.3.11 indicates that 0.001 % of the total variations are not satisfactorily explained by the model. It is proved from that table that $F_{\text{statistics}}$ value for entire model is higher. This large value means that % biosorption can be adequately explained by the model equation. Generally, P values lower than 0.05 indicates that the model is considered to be statistically significant at 95% confidence level. The % biosorption prediction from the model is shown in table-6.

It is implied from table-7 that all the squared terms of all the variables and the linear terms are significant ($P < 0.05$). Among the interaction terms, all the terms ($P < 0.05$) are insignificant on the biosorption capacity. Fig. 13 and Fig. 14 shows pareto chart and normal probability plot

(NPP) of residual values. It could be seen that the experimental points are reasonably aligned suggesting normal distribution.

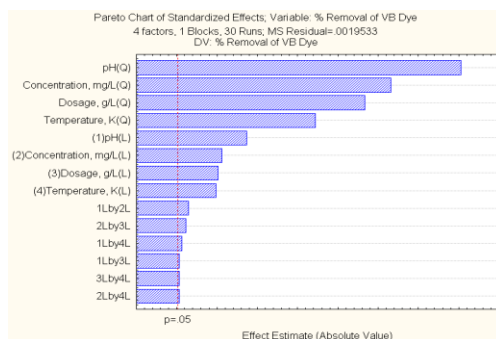


Figure 13: Pareto Chart

The optimal set of conditions for maximum percentage biosorption of VB dye is pH = 5.1273, initial VB dye concentration = 19.4355 mg/L, biosorbent dosage = 31.1997 g/L, and temperature = 304.4728 K. The extent of biosorption of VB dye at these optimum conditions was 92.2763 %. It is evident that experimental values of % biosorption are in close agreement with that of predicted by Central Composite Design. Experiments are conducted in triplicate with the above predicted optimal set of conditions and the % biosorption of VB dye is 92 %, which is closer to the predicted % biosorption.

Interaction effects of biosorption variables:

The three-dimensional view of response surface contour plots [Fig. 15 to 20] show % biosorption as a function of for various combinations of independent variables. The plots are represented as a function of two factors at a time keeping other factors fixed at zero level.

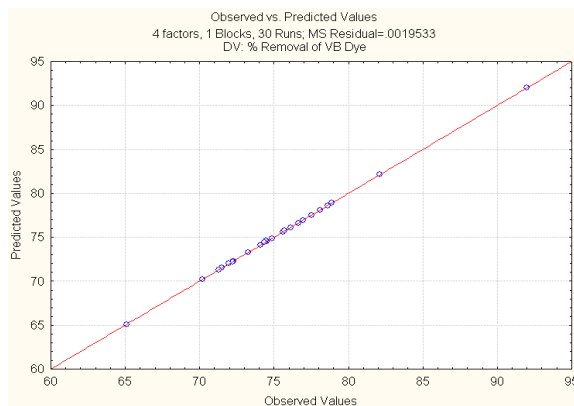


Figure 14: Normal probability plot for % biosorption of VB dye

It is found from the response surface plots that the % biosorption is maximal at low and high levels of the input variables. However, there exists a region where neither an increasing nor a decreasing trend in % biosorption is observed. The biosorption variables should be optimum to maximize the % biosorption. The % biosorption of VB dye is strongly influenced by the pH as

evident from figs. 15 and 16.

The predicted optimal set of conditions for percentage biosorption of VB dye is

pH of aqueous solution = 6.1273

Initial VB dye concentration = 19.4355 mg/L

Biosorbent dosage = 31.1997 g/L

Temperature = 304.4728 K

% biosorption of VB dye = 92.2763

The optimal set of conditions obtained with CCD are shown in table-7 along with experimental values.

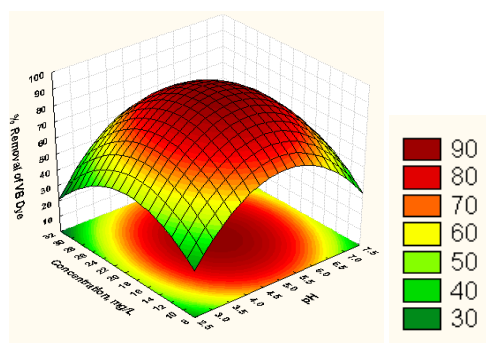


Figure 15: Surface contour plot for the effects of pH and initial VB dye concentration on % biosorption

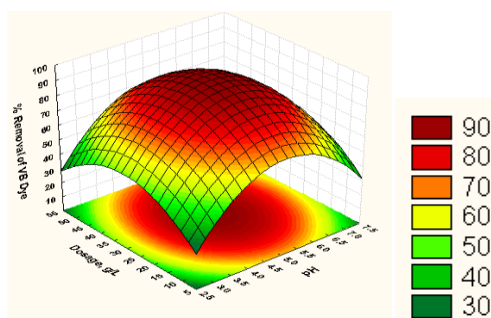


Figure 16: Surface contour plot for the effects of pH and dosage on % biosorption of VB dye

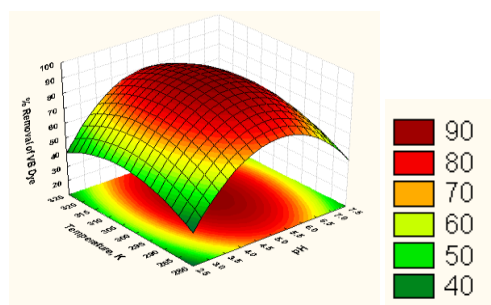


Figure 17: Surface contour plot for the effects of pH and Temperature on % biosorption of VB dye

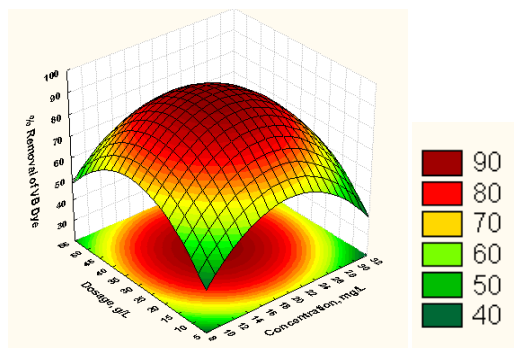


Figure 18: Surface contour plot for the effects of initial concentration and dosage on % biosorption of VB dye

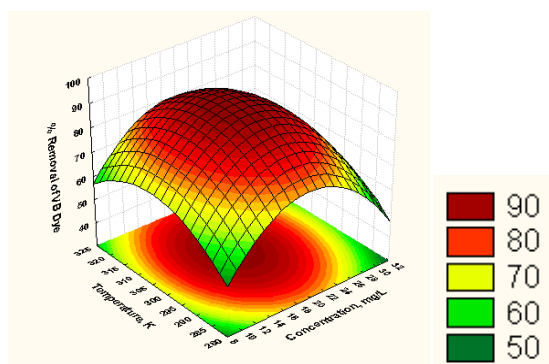


Figure 19: Surface contour plot for the effects of initial concentration and Temperature on % biosorption of VB dye

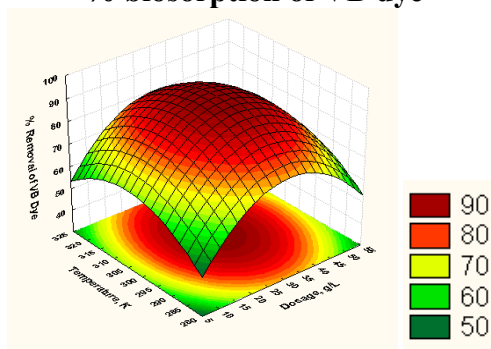


Figure 20: Surface contour plot for the effects of Dosage and Temperature on % biosorption of VB dye

Table 7: Comparison between optimum values from CCD and experimentation

Variable	CCD	Experimental value
pH of aqueous solution	6.1273	6
Initial VB concentration, mg/L	19.4355	20
Biosorption dosage, w, g/L	31.1997	30
Temperature, K	304.4728	303
% biosorption	92.2763	92.0

Characterization of *Jania rubens* red algae Fourier Transform Infra-Red Spectroscopy (FTIR)

Infrared spectroscopy belongs to the group of molecular vibrational spectroscopies which are molecule-specific and give direct information about the functional groups, their kind, interactions and orientations. Its sampling requirements allow the gain of information from liquids and gases and in particular from solid surfaces. Even if historically IR has been mostly used for qualitative analysis, to obtain structural information, nowadays instrumental evolution makes non-destructive and quantitative analysis possible [36-37] with significant accuracy and precision. The shift of the bands and the changes in signal intensity allow the identification of the functional groups involved in dye sorption.

FTIR spectrum of untreated VB dye:

The FTIR spectrum presented in the figure 21 below indicates the presence of Amine C-N stretch at a band of 1296.02721 cm⁻¹, and the peak at the band width of 1440.6731 cm⁻¹ attributed to the presence of methylene group of lipids. The anti symmetric stretching of RCOOH- is observed at band width of 1579.53316 cm⁻¹, at the band width of 2497.5524 cm⁻¹ Amine stretch of N-H is observed, the presence of -OH stretch is confirmed at the peaks of 3479.2159 and 3521.64363 cm⁻¹.

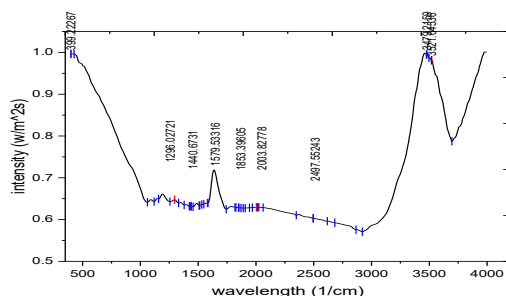


Figure 21: FTIR spectrum of VB dye untreated *Jania Rubens* red algae

FTIR spectrum of VB dye treated with *Jania rubens* red algae:

The peak presented in the FTIR spectrum figure 22 given below at 1355.8141 cm⁻¹ indicates the presence of Amine C-N stretch, Also the (C=O) asymmetric stretching is observed at a wavelength of 1569.8901 cm⁻¹, the wavelength at 2217.9037 attributes to the presence of Alkynes stretching, The amine N-H stretching is observed at the wavelengths of 2377.97844, 2514.90994, 2620.98359, 2748.27198 cm⁻¹, the presence of -OH bond is confirmed at the peak with the corresponding wavelength of 3479.2159 cm⁻¹.

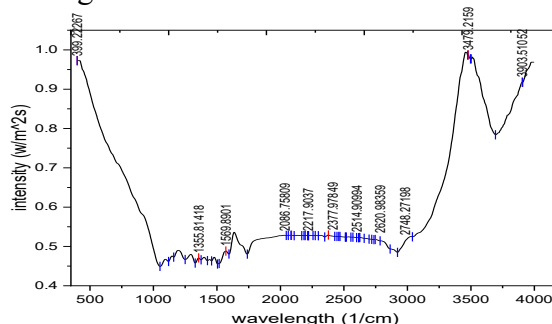


Figure 22: FTIR spectrum of VB dye treated *Jania rubens* red algae

Table 8: Shift of FTIR peaks for untreated and *Jania Rubens* red algae treated VB dye

S/N	3A (Peak) cm^{-1}	3C (peak) cm^{-1}	Description
1	399.2267	399.2267	
2	1296.02721	1355.8141	Amine (C-N) stretching
3	1440.6731	-	Methylene group of lipids
4	1579.53316	1569.8901	Anti symmetric stretching of RCOO^- (Carboxylate ion)
5	1853.39605	-	
6	2003.82778	-	
7	-	2086.75809	
8	2217.9037	-	Alkynes stretch
9	2497.55243	2377.97849	Amine N-H stretch
10	-	2514.9099	
11	-	2620.98354	
12	-	2748.27198	
13	3497.2159	3497.2159	-OH stretch
14	3521.64536	-	
15	-	3903.51052	

X-Ray Diffraction:

The X-Ray Diffractograms (XRD) of the powder samples are taken using a RigakuUltima model IV. The diffracted X-ray intensities are recorded as a function of 2α by using copper target (Cu-K α radiation with wave length, $\alpha = 1.5492 \text{ \AA}$) at a scan speed of $2^\circ/\text{min}$. XRD patterns are recorded from 3° to 90° . Different phases of the samples are to be identified by comparing with a set of d'values and the corresponding intensities with the standards from the ICDD (International Center for Diffraction Data) files.

XRD for VB dye untreated with *Jania rubens* red algae

XRD patterns of untreated powder are shown in figs 23 and 24. XRD patterns shown in figs 23 and 24 do not indicate sharp peaks, less crystallinity and exhibit little amorphous nature. The XRD data shows the peaks at the 2θ values of 45.33, 45.71, 45.86, 45.96, 46.28, 46.51, 46.90, 47.20 corresponds to the C60. 2 S8 (beta, 90 K), 1,2-Bis-crown-5-calix [4] arene, 2C70, 3CS2 solvate, I24 O192 Si96, Na2 O5 Si2, C15 Br3 Cu3 F18 N6, As19 Pb4 S68 Sb21 Tl8 and High-Spin cisBis(acetonitrile)Tetrakis (triphenylphosphine oxide) iron(II) Triiodide--Acetonitrile (C78 H69 Fe I6 N3 O4 P4). Their d values are 1.999, 1.9832, 1.97712, 1.97305, 1.96015, 1.95099, 1.93867 and 1.92407. The miller indices(h k l) are (-1 0 1), (1 0 1), (1 1 1), (-1 2 1), (1 2 1), (1 11 0), (2 3 0) and (0 7 1) respectively[38-39].

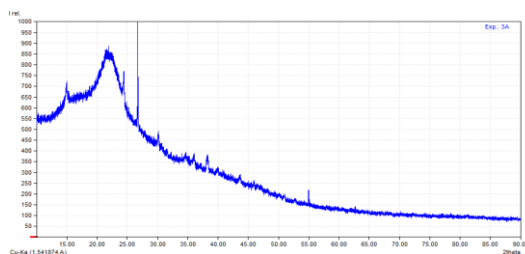


Figure 23: XRD pattern of VB dye untreated *Jania rubens* red algae

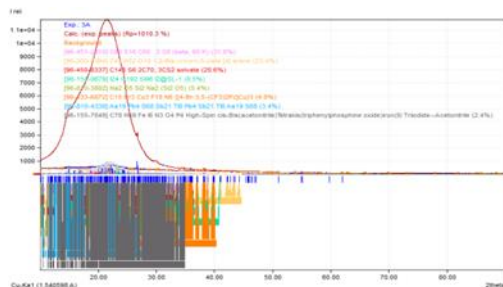


Figure 24: XRD pattern of VB dye untreated *Jania Rubens* red algae with matching compounds

XRD for VB dye treated with *Jania Rubens* red algae

XRD patterns for treated powder [Figs. 25 and 26] exhibit good crystallinity, more amorphous nature and increase in surface area and porosity. The changes in 2θ values and compounds for before and after indicate that biosorption has occurred.

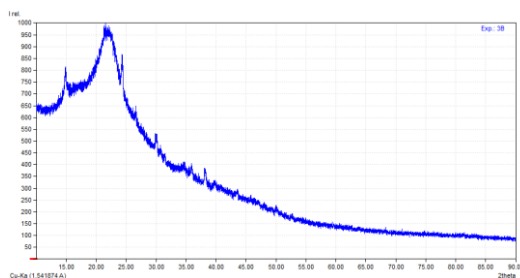


Figure 25: XRD pattern of VB dye treated *Jania rubens* red algae

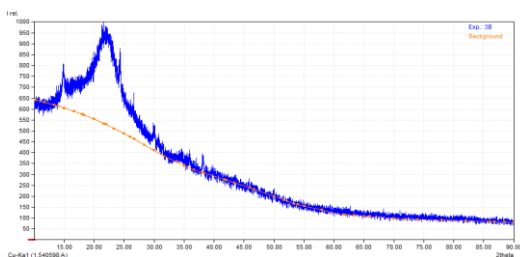


Figure 26: XRD pattern of VB dye treated *Jania rubens* red algae with matching compounds

Conclusion

The aim of the study was to determine the suitability of *Jania rubens* sorbent for the removal of VB dye from aqueous solutions. The equilibrium agitation time for VB dye sorption is 40 minutes. Percentage sorption of VB dye from the aqueous solution increases significantly with increase in pH from 2 (49 %) to 5 (72 %). The optimum dosage for sorption is 30 g/L (1.75 mg/g). The maximum uptake capacity of 0.597 mg/g is obtained at 303 K. The maximum sorption of VB dye (92.2763 %) onto *Jania Rubens* is observed when the processing parameters are set as: pH = 5.1273, w = 31.1997 g/L, Co = 19.4355 mg/L and T = 304.4728 K using CCD. The thermodynamic data show that % sorption of IC dye is increased with increase in temperature. The investigation also reveals the endothermic nature of sorption as ΔH is positive (3872.509), irreversible nature of sorption as ΔS is positive (0.9956) and spontaneity of sorption as indicated by negative ΔG ($\Delta G = -3570.827$ J/mole).

References

1. VadaliPrمود, Ch. Asha Immanuel Raju, K.V.D. Pratyusha, P. RatnaRaju, and P. VenkataRao. Studies on biosorption of ricinuscommunis powder for the removal of congo red dye 2018 JETIR October 2018, Volume 5, Issue 10.
2. G.Prasad, Prof MeenaVangalapati, Dr.Ch.A.I.Raju. Isothermal and kinetics of biosorption capacity of amido black dye using chaetomorpha antennina green algae powder and optimization using central composite design. Vol 7, issue 01, 2020.
3. Volesky, B., 1990a. "Biosorption of Heavy Metals". CRC Press, Boca Raton, FL.
4. Niu, H., Volesky, B., 2003a. " Biosorption mechanism for anionic metal species with waste crab shells. Hydrometallurgy 71 (1-2), 209-215.
5. S. N. B. S. Jaafar, 2006. Dye removal using clay. Adsorption study, Faculty of Chemical Engineering and Natural Resources. University College of Engineering & Technology Malaysia degree of Bachelor of Chemical Engineering.
6. Arnaud Boivin, Richard Cherrier, Corinne Perrin-Ganier, Michel Schiavon, —Time effect on bentazone sorption and degradation in soil, pest Management science, 60(8)(2004) 809-814.
7. A.M. Elgarahy, K.Z. Elwakeel, S.H. Mohammad, G.A. Elshoubaky. A critical review of biosorption of dyes, heavy metals and metalloids from wastewater as an efficient and green process. Cleaner Engineering and Technology. July 2021.
8. Fatih Deniz. Dye removal by almond shell residues: Studies on biosorption performance and process design. Materials Science and Engineering C. March 2013.
9. A.E. Ofomaja, E.B. Naidoo. Biosorption of lead(II) onto pine cone powder: Studies on biosorption performance and process design to minimize biosorbent mass. Carbohydrate Polymers. 2010.
10. Thomas H. Christensen; Cadmium soil sorption at low concentrations: I. Effect of time, cadmium load, pH, and calcium; Water, Air, and Soil Pollution volume 21, pages 105–114 (1984).

11. N. S. Bolan, n. J. Barrow, a. M. Posner,; Describing the effect of time on sorption of phosphate by iron and aluminium hydroxides; *Journal of Soil Science*; Volume 36, Issue 2; 1985; Pages 187-197.
12. Chidozie Charles Nnaji, s. C. Emefu; Effect of Particle Size on the Sorption of Lead from Water by Different Species of Sawdust: Equilibrium and Kinetic Study; April 2017; *Bioresources* 12(2):4123-4145.
13. Hao Wang; Farhang Shadman; Effect of Particle Size on the Adsorption and Desorption
14. Properties of Oxide Nanoparticles; May 2013; *AIChE Journal* 59(5).
15. Guillaume Echevarria, Marsha ISheppard, JeanLouis Morel; Effect of pH on the sorption of uranium in soils; *Journal of Environmental Radioactivity*; Volume 53, Issue 2, March 2001, Pages 257-264.
16. XIONG, Chunhua, LIU, Xiaozheng, YAO, Caiping; Effect of pH on sorption for RE(III) and sorption behaviors of Sm(III) by D152 resin; *Journal of Rare Earths*; Volume 26, Issue 6, December 2008, Pages 851-856.
17. Yangyang Guo, Yuran Li, Tingyu Zhu, and Meng Ye; Effects of Concentration and Adsorption Product on the Adsorption of SO₂ and NO on Activated Carbon; *Energy Fuels* 2013, 27, 1, 360–366.
18. Washington J. Braida, Jason C. White, Francis J. Ferrandino, and Joseph J. Pignatello; Effect of Solute Concentration on Sorption of Polyaromatic Hydrocarbons in Soil: Uptake Rates; *Environ. Sci. Technol.* 2001, 35, 13, 2765–2772.
19. Meenakshi, S., C. Sairam Sundaram, and Rugmini Sukumar. "Enhanced fluoride sorption by mechanochemically activated kaolinites." *Journal of hazardous materials* 153, no. 1-2 (2008): 164-172.
20. Dalton, Chad R., and Bruno C. Hancock. "Processing and storage effects on water vapor sorption by some model pharmaceutical solid dosage formulations." *International journal of pharmaceuticals* 156, no. 2 (1997): 143-151.
21. Ten Hulscher, Th EM, and Gerard Cornelissen. "Effect of temperature on sorption equilibrium and sorption kinetics of organic micropollutants-a review." *Chemosphere* 32, no. 4 (1996): 609-626.
22. Iglesias, H. A., and J. Chirife. "Prediction of the effect of temperature on water sorption isotherms of food material." *International Journal of Food Science & Technology* 11, no. 2 (1976): 109-116.
23. Kim, Cha Young, Hyung-Min Choi, and Hyeon Tae Cho. "Effect of deacetylation on sorption of dyes and chromium on chitin." *Journal of applied polymer science* 63.6 (1997): 725-736.
24. Inbaraj, B. S., Chien, J. T., Ho, G. H., Yang, J., & Chen, B. H. (2006). Equilibrium and kinetic studies on sorption of basic dyes by a natural biopolymer poly (γ -glutamic acid). *Biochemical Engineering Journal*, 31(3), 204-215.

25. Wang, J., Liu, X., Liu, G., Zhang, Z., Wu, H., Cui, B., ...& Zhang, W. (2019). Size effect of polystyrene microplastics on sorption of phenanthrene and nitrobenzene. *Ecotoxicology and environmental safety*, 173, 331-338.
26. Tikhomirova, T. I., Ramazanov, G. R., & Apyari, V. V. (2018). Effect of nature and structure of synthetic anionic food dyes on their sorption onto different sorbents: Peculiarities and prospects. *Microchemical Journal*, 143, 305-311.
27. Riyasudheen, N., Binsy, P., Aswini, K. K., Jayadevan, J., & Athiyathil, S. (2012). Bovine serum albumin immobilized-polyvinyl alcohol membranes: A study based on sorption, dye release and protein adsorption. *Polymer-Plastics Technology and Engineering*, 51(13), 1351-1354.
28. Berlin, M., & Kumar, G. S. (2018). Numerical modelling on sorption kinetics of nitrogen species in wastewater-applied agricultural field. *Applied Water Science*, 8(8), 1-16.
29. Ho, Y. S., & McKay, G. (1998). The kinetics of sorption of basic dyes from aqueous solution by sphagnum moss peat. *The Canadian journal of chemical engineering*, 76(4), 822-827.
30. Ho, Y. S., & McKay, G. (2003). Sorption of dyes and copper ions onto biosorbents. *Process Biochemistry*, 38(7), 1047-1061.
31. Ho, Y. S., & McKay, G. (1999). Pseudo-second order model for sorption processes. *Process biochemistry*, 34(5), 451-465
32. Gamoudi, S., & Srasra, E. (2019). Adsorption of organic dyes by HDPy⁺-modified clay: effect of molecular structure on the adsorption. *Journal of Molecular Structure*, 1193, 522-531.
33. Asgher, Mahwish, and Haq Nawaz Bhatti. "Evaluation of thermodynamics and effect of chemical treatments on sorption potential of Citrus waste biomass for removal of anionic dyes from aqueous solutions." *Ecological Engineering* 38, no. 1 (2012): 79-85.
34. Mahmoud, Mohamed Ahmed. "Oil spill cleanup by raw flax fiber: Modification effect, sorption isotherm, kinetics and thermodynamics." *Arabian Journal of Chemistry* 13, no. 6 (2020): 5553-5563.
35. Vyavahare, G., Jadhav, P., Jadhav, J., Patil, R., Aware, C., Patil, D., ...& Gurav, R. (2019). Strategies for crystal violet dye sorption on biochar derived from mango leaves and evaluation of residual dye toxicity. *Journal of cleaner production*, 207, 296-305.
36. Netto, M. S., da Silva, N. F., Mallmann, E. S., Dotto, G. L., & Foletto, E. L. (2019). Effect of salinity on the adsorption behavior of methylene blue onto comminuted raw avocado residue: CCD-RSM design. *Water, Air, & Soil Pollution*, 230(8), 1-17.
37. Kim, C. Y., Choi, H. M., & Cho, H. T. (1997). Effect of deacetylation on sorption of dyes and chromium on chitin. *Journal of applied polymer science*, 63(6), 725-736.
38. Dhal, J. P., Sethi, M., Mishra, B. G., & Hota, G. (2015). MgO nanomaterials with different morphologies and their sorption capacity for removal of toxic dyes. *Materials Letters*, 141, 267-271.

39. Tehrani-Bagha, A. R., Nikkar, H., Mahmoodi, N. M., Markazi, M., & Menger, F. M. (2011). The sorption of cationic dyes onto kaolin: Kinetic, isotherm and thermodynamic studies. *Desalination*, 266(1-3), 274-280.
40. Zhu, M. X., Li, Y. P., Xie, M., & Xin, H. Z. (2005). Sorption of an anionic dye by uncalcined and calcined layered double hydroxides: a case study. *Journal of hazardous materials*, 120(1-3), 163-171.